Supporting Information

Realizing CO-Free Pathway and Boosting Durability on Highly Dispersed Cu-Doped PtBi Nanoalloys towards Methanol Full Electrooxidation

Fengling Zhao[a], JinYu Ye[c], Qiang Yuan[*a, b], Xiaotong Yang[a] and Zhiyou Zhou[c]

[a]State Key Laboratory Breeding Base of Green Pesticide and Agricultural Bioengineering, Key Laboratory of Green Pesticide and Agricultural Bioengineering (Ministry of Education), State-Local Joint Laboratory for Comprehensive Utilization of Biomass, Center for R&D of Fine Chemicals, College of Chemistry and Chemical Engineering, Guizhou University, Guiyang, Guizhou Province 550025, People's Republic of China.

[b]Key Lab of Organic Optoelectronics & Molecular Engineering, Tsinghua University, Beijing 100084, People's Republic of China.

[c]State Key Laboratory of Physical Chemistry of Solid Surfaces, College of Chemistry and Chemical Engineering, Xiamen University, Xiamen 361005, People's Republic of China.

*Corresponding author e-mail: qyuan@gzu.edu.cn

1. Experimental section

1.1 materials

Platinum(II) acetylacetonate ($Pt(acac)_2$, AR), Bismuth nitrate pentahydrate ($Bi(NO_3)_3{\cdot}5H_2O$, AR), Copper(II) acetylacetonate ($Cu(acac)_2$, AR), Polyvinylpyrrolidone (PVP-8000) were purchased from Sigma-Aldrich. NaI (AR), N,N-Dimethylformamide (DMF, 99.8%), absolute methanol/ethanol, KOH (AR), $HClO_4$ (AR), dimethyl sulfoxide (DMSO, 99.5%) and Deuterium oxide (D_2O, AR) were got from Aladdin. Pt black was obtained from Johnson Matthey.

1.2 Measurement of electrocatalytic performance

Cyclic voltammetry (CV) and i-t measurements were tested in a typical

three-electrode cell equiped with salt bridge and controlled by CHI 760E electrochemical workstation (CHI Instruments, Shanghai, Chenhua Co., Ltd.). The super pure water (18.25 MΩ cm) was used as solvent and purified through a Milli-Q Lab system (Nihon Millipore Ltd.). The glassy carbon (GC, Φ=5 mm) embedded into a Teflon holder was a working electrode. Prior to an electrochemical test, the GC electrode was mechanically polished using alumina powder (50 nm). It was then cleaned in an ultrasonic bath for 5 minutes. Then took a certain amount of catalysts to disperse with the volume ratio (1:1) of super pure water and ethanol under ultrasonic bath. The suspension of nanocrystals was spread on the GC electrode, and the metal loading amount of nanocrystals was controlled at geometric area of 10.2-12.7 μg Pt per cm^2. When the electrode was dried under infrared lamp, 5.0 μl of Nafion diluents (0.1wt.% Nafion® solution) was coated onto the electrode surface. The Ag/AgCl electrode and platinum foil were used as the reference and counter electrode, respectively. The CVs were recorded in nitrogen-saturated 0.5 M KOH solution or 0.5 M KOH + 1 M methanol solution and the potential was scanned from -0.8 to 0.2 V (vs. Ag/AgCl), and the scan rate was 50 mV s^{-1}.

The ECSAs were estimated by CO stripping: All samples were carried out by firstly in the N_2-saturated 0.1 M $HClO_4$ solution electrolytic cell to test from -0.25 to 0.9 V (vs. Ag/AgCl) at a scan rate of

50 mV s^{-1}, then inlet CO untill saturation and recorded the CVs. The ECSA was calculated by the following equation:

$$ECSA = Q/(0.42 \times M),$$

where Q (mC) is the charge for the CO adsorption. 0.42 (mC/cm^2) is the electrical charge associated with full monolayer adsorption of CO on Pt.

In situ anti-CO poisoning testing: The testing was carried out in 0.5 M KOH + 1 M CH_3OH solution. Before performed CVs, CO gas was first inputted with a flow rate of 17.8 mL/min for 10 minutes, then kept CO inputting and CV scanning was performed.

The d-band centers of the $Pt_{69.2}Bi_{29.6}Cu_{1.2}$ nanoalloy and commercial Pt black were calculated from the following equation[1-5] based on the valence band spectra. The d-band center positions of Pt of the $Pt_{69.2}Bi_{29.6}Cu_{1.2}$ nanoalloy and commercial Pt black were respectively located at -4.37 eV and -3.77 eV, revealing that d-band center of Pt of the $Pt_{69.2}Bi_{29.6}Cu_{1.2}$ nanoalloy downshifted compared with pure Pt black. [1-5]

$$d-band\ center = -\int_{-2eV}^{10eV}[binding\ energy(E)\times intensity(E)]dE \Big/ \int_{-2eV}^{10eV} intensity(E)dE$$

1 Y. W. Lee, H. Ahn, S. E. Lee, H. Woo, S. W. Han, Fine Control over the Compositional Structure of Trimetallic Core-Shell Nanocrystals for Enhanced Electrocatalysis, *ACS Appl. Mater. Interfaces*, 2019, **11**, 25901-25908.

2 S. J. Yoo, S. K. Kim, T. Y. Jeon, J. G. Lee, S. C. Lee, K. S. Lee, Y. H. Cho, Y. E. Sung, T. H. Lim, Enhanced stability and activity of Pt-Y alloy catalysts for electrocatalytic oxygen reduction, *Chem. Commun*., 2011, **47**, 11414-11416.

3 B. S. Mun, M. Watanabe, M. Rossi, V. Stamenkovic, N. M. Markovic, P. N. Ross, A

study of electronic structures of Pt_3M (M=Ti, V, Cr, Fe, Co, Ni) polycrystalline alloys with valence-band photoemission spectroscopy, *J. Chem. Phys*., 2005, **123**, 204717.

4 M. T. Gorzkowski, A. Lewera, Probing the Limits of d-Band Center Theory: Electronic and Electrocatalytic Properties of Pd-Shell-Pt-Core Nanoparticles, *J. Phys. Chem. C*, 2015, **119**, 18389-18395.

5 T. Hofmann, T. H. Yu, M. Folse, L. Weinhardt, M. Bär, Y. f. Zhang, B. V. Merinov, D. J. Myers, W. A. Goddard, C. Heske, Using Photoelectron Spectroscopy and Quantum Mechanics to Determine d-Band Energies of Metals for Catalytic Applications, *J. Phys. Chem. C*, 2012, **116**, 24016-24026.

Table S1. A summary of the durability on electrocatalyst toward MOR. (All data obtained at room temperature; A. R. stands for activity retention.)

Electrocatalyst	Electrolyte	Durability	Reference
$Pt/Ni(OH)_2/rGO$	1 M KOH + 1 M CH_3OH	90 % A. R. after 3,600 s 40 % A. R. after 50,000 s	[6]Nat. Commun., 2015, 6, 10035.
Pt_2Bi	1M NaOH + 1 M CH_3OH	58.4 % A. R. after 10,000 s	[7]Nano Res., 2019, 12, 429-436.
Pt-Bi/GNs	1 M KOH + 1 M CH_3OH	50.5 % A. R. after 2,000 s	[8]Electrochim. Acta, 2018, 264, 53-60.
PtAu/RGO/GC	1 M KOH + 1 M CH_3OH	20 % A. R. after 4,000 s	[9]J. Mater. Chem. A, 2013, 1, 7255-7261.
$Pt_{0.5}Ag/C$	0.5 M KOH + 2 M CH_3OH	32.7 % A. R. after 3,600 s	[10]J. Catal., 2012, 290, 18-25.
PtCu NFs	0.5 M KOH + 1 M CH_3OH	38.8 % A. R. after 3,000 s	[11]Adv. Mater., 2016, 28, 8712-8717
PtRu NWs	0.1 M $HClO_4$ + 0.5 M CH_3OH	29.9 % A. R. after 4,000 s	[12]J. Am. Chem. Soc., 2018, 140, 1142-1147
Pt_7Ru_2Fe NW	0.1 M $HClO_4$ + 0.5 M CH_3OH	116.3 % A. R. after 3,600 s	[13]Energy Environ. Sci., 2015, 8, 350-363
$Fe_{28}Pt_{38}Pd_{34}$ NWs	0.1 M $HClO_4$ + 0.2 M CH_3OH	55 % A. R. after 7,200 s	[14]J. Am. Chem. Soc., 2011, 133, 15354-15357.
$Pt_{69}Ni_{16}Rh_{15}$	0.1 M $HClO_4$ + 0.5M CH_3OH	29 % A. R. after 5,000 s	[15]Adv. Mater., 2019, 31, 1805833
$Pt_{94}Zn_6$ NWs	0.1 M $HClO_4$ + 0.2 M CH_3OH	37 % A. R. after 3,000 s	[16]Nano Res., 2019, 12, 1173-1179
PtNi	0.5M H_2SO_4 + 0.5M CH_3OH	43 % A. R. after 3,600 s	[17]Adv. Funct. Mater., 2018, 28, 1704774
3D Pt_3Co NWs	0.5 M H_2SO_4 + 0.5 M CH_3OH	40 % A. R. after 2,000 s	[18] Angew. Chem. Int. Ed., 2015, 54, 3797-3801.
Pt/SiC	0.5M H_2SO_4 + 0.5M CH_3OH	46 % A. R. after 6,000 s	[19]Small, 2019, 15, 1902951
PtCoNiRh NWs/C	0.1 M $HClO_4$ + 0.5 M CH_3OH	52% A. R. after 10,000 s	[20]Nano Energy, 2020, 71, 104623
PtRu/PC–H	0.1 M $HClO_4$ + 0.5 M CH_3OH	16.3 % A. R. after 7,200 s	[21]Appl. Catal. B-Environ., 2020, 263, 118345
$Pt_{69.2}Bi_{29.6}Cu_{1.2}$	0.5 M KOH + 1 M CH_3OH	161.4% A. R. after 3,600s 202.7% A. R. after 36,000s 166.4 % A. R.after108,000s	This work

Note: In table S1, all initial currents were obtained at 30 s as the reference. Within 30s, because of the double-layer discharge of the electrodes and the oxidation of adsorbed hydrogen, the current decreases rapidly. To avoid this phenomenon and heavy fluctuation of the current, we chose the current at 30s as the initial current for reference to calculate activity retention.

6 W. J. Huang, H. T. Wang, J. G. Zhou, J. Wang, P. N. Duchesne, D. Muir, P. Zhang, N. Han, F. P. Zhao, M. Zeng, J. Zhong, C. H. Jin, Y. G. Li, S. T. Lee, H. J. Dai, Highly active and durable methanol oxidation electrocatalyst based on the synergy of platinum-nickel hydroxide-graphene, *Nat. Commun*., 2015, **6**, 10035.

7 X. L. Yuan, X. J. Jiang, M. H. Cao, L. Chen, K. Q. Nie, Y. Zhang, Y. Xu, X. H. Sun, Y. G. Li, Q. Zhang, Intermetallic PtBi core/ultrathin Pt shell nanoplates for efficient and stable methanol and ethanol electro-oxidization, *Nano Res*., 2019, **12**, 429-436.

8 Z. S. Li, S. H. Xu, Y. X. Xie, Y. L. Wang, S. Lin, Promotional effects of trace Bi on its highly catalytic activity for methanol oxidation of hollow Pt/graphene catalyst, *Electrochim. Acta*, 2018, **264**, 53-60.

9 F. F. Ren, C. Q. Wang, C. Y. Zhai, F. X. Jiang, R. R. Yue, Y. K. Du, P. Yang, J. K. Xu, One-pot synthesis of a RGO-supported ultrafine ternary PtAuRu catalyst with high electrocatalytic activity towards methanol oxidation in alkaline medium, *J. Mater. Chem. A*, 2013, **1**, 7255-7261.

10 Y. Y. Feng, L. X. Bi, Z. H. Liu, D. S. Kong, Z. Y. Yu, Significantly enhanced electrocatalytic activity for methanol electro-oxidation on Ag oxide-promoted PtAg/C catalysts in alkaline electrolyte, *Journal of Catalysis*, 2012, **290**, 18-25.

11 Z. C. Zhang, Z. M. Luo, B. Chen, C. Wei, J. Zhao, J. Z. Chen, X. Zhang, Z. C. Lai, Z. X. Fan, C. L. Tan, M. T. Zhao, Q. P. Lu, B. Li, Y. Zong, C. C. Yan, G. X. Wang, Z. C. J. Xu, H. Zhang, One-Pot Synthesis of Highly Anisotropic Five-Fold-Twinned PtCu Nanoframes Used as a Bifunctional Electrocatalyst for Oxygen Reduction and Methanol Oxidation, *Adv. Mater*., 2016, **28**, 8712-8717.

12 L. Huang, X. P. Zhang, Q. Q. Wang, Y. J. Han, Y. X. Fang, S. J. Dong,

Shape-Control of Pt-Ru Nanocrystals: Tuning Surface Structure for Enhanced Electrocatalytic Methanol Oxidation, *J. Am. Chem. Soc*., 2018, **140**, 1142-1147.

13 M. E. Scofield, C. Koenigsmann, L. Wang, H. Q. Liu, S. S. Wong, Tailoring the composition of ultrathin, ternary alloy PtRuFe nanowires for the methanol oxidation reaction and formic acid oxidation reaction, *Energy Environ. Sci.*, 2015, **8**, 350-363.

14 S. J. Guo, S. Zhang, X. L. Sun, S. H. Sun, Synthesis of Ultrathin FePtPd Nanowires and Their Use as Catalysts for Methanol Oxidation Reaction, *J. Am. Chem. Soc*., 2011, **133**, 15354-15357.

15 W. Y. Zhang, Y. Yang, B. L. Huang, F. Lv, K. Wang, N. Li, M. C. Luo, Y. G. Chao, Y. J. Li, Y. J. Sun, Z. K. Xu, Y. N. Qin, W. X. Yang, J. H. Zhou, Y. P. Du, D. Su, S. J. Guo, Ultrathin PtNiM (M = Rh, Os, and Ir) Nanowires as Efficient Fuel Oxidation Electrocatalytic Materials, *Adv. Mater*., 2019, **31**, 1805833.

16 Y. C. Xu, X. Q. Cui, S. T. Wei, Q. H. Zhang, L. Gu, F. Meng, J. C. Fan and W. T. Zheng, Highly active zigzag-like Pt-Zn alloy nanowires with high-index facets for alcohol electrooxidation, *Nano Res.*, 2019, **12**, 1173-1179.

17 P. P. Yang, X. L. Yuan, H. C. Hu, Y. L. Liu, H. W. Zheng, D. Yang, L. Chen, M. H. Cao, Y. Xu, Y. L. Min, Y. G. Li and Q. Zhang, Solvothermal Synthesis of Alloyed PtNi Colloidal Nanocrystal Clusters (CNCs) with Enhanced CatalyticActivity for Methanol Oxidation, *Adv. Funct. Mater*., 2018, **28**, 1704774.

18 B. Xia, H. Wu, N. Li, Y. Yan, X. W. Lou, X. Wang, One-Pot Synthesis of Pt-Co Alloy Nanowire Assemblies with Tunable Composition and Enhanced Electrocatalytic Properties, *Angew. Chem. Int. Ed*., 2015, **54**, 3797-3801.

19 G. L. Bai, C. Liu, Z. Gao, B. Y. Lu, X. L.Tong, X. Y. Guo and N. J. Yang, Atomic Carbon Layers Supported Pt Nanoparticles for Minimized CO Poisoning and Maximized Methanol Oxidation, *Small*, 2019, **15**, 1902951.

20 W. Wang, X. W. Chen, X. Zhang, J. Y. Ye, F. Xue, C. Zhen, X. Y. Liao, H. Q. Li, P. T. Li, M. C. Liu, Q. Kuang, Z. X. Xie, S. F. Xie, Quatermetallic Pt-Based Ultrathin Nanowires Intensified by Rh Enable Highly Active and Robust Electrocatalysts for Methanol Oxidation, *Nano Energy*, 2020, **71**, 104623.

21 J. M. Zhang, X. M. Qu, Y. Han, L. F. Shen, S. H. Yin, G. Li, Y. X. Jiang, S. G.

Sun, Engineering PtRu bimetallic nanoparticles with adjustable alloying degree for methanol electrooxidation: Enhanced catalytic performance, *Appl. Catal. B-Environ.*, 2020, **263**, 118345.

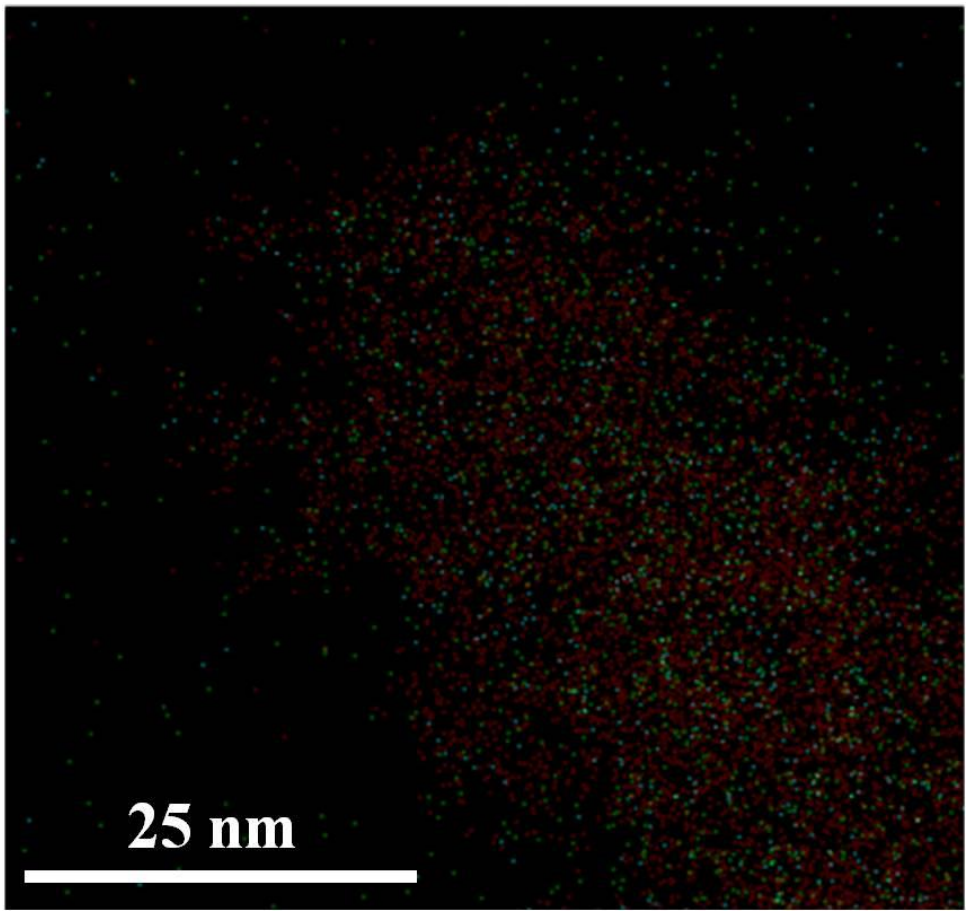

Fig. S1 The overlaps of Pt, Bi and Cu.

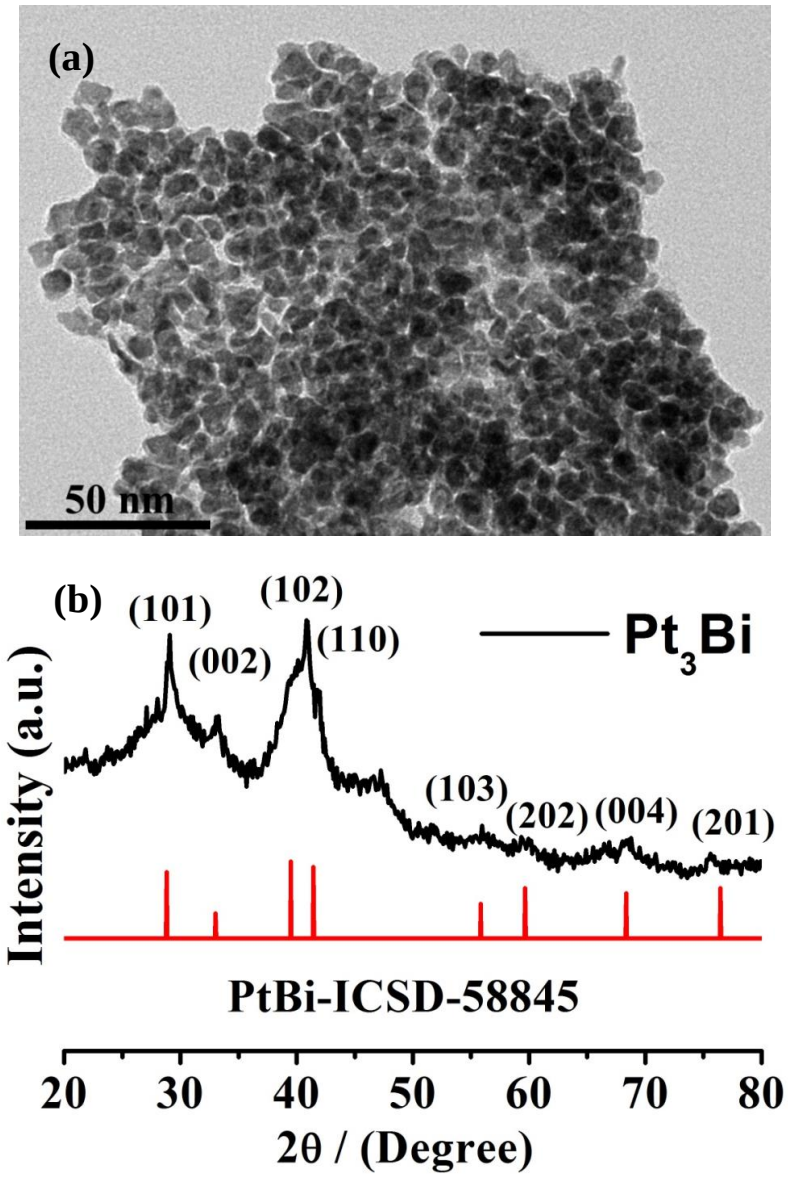

Fig. S2 TEM images (a) and XRD pattern (b) of the synthesized intermetallic Pt_3Bi nanocrystals. (The atomic ratio of Pt:Bi analyzed by ICP-OES was 75:25, marked as Pt_3Bi; The shape and size of intermetallic Pt_3Bi nanocrystal is similar with that of $Pt_{69.2}Bi_{29.6}Cu_{1.2}$ nanoalloy.)

We can see that the XRD pattern of the synthesized Pt_3Bi nanocrystal is consistent with the standard spectrum of intermetallic compound (PtBi-ICDS-58845), and when PtBi nanocrystal was synthesized, the intermetallic phase is usually formed. [7, 22-25]

22 B. W. Zhang, W. H. Lai, T. Sheng, X. M. Qu, Y. X. Wang, L. Ren, L. Zhang, Y.

Du, Y. X. Jiang, S. G. Sun and S. X. Dou, Ordered platinum-bismuth intermetallic clusters with Pt-skin for a highly efficient electrochemical ethanol oxidation reaction, *J. Mater. Chem. A*, 2019, **7**, 5214-5220.

23 Y. N. Qin, M. C. Luo, Y. J. Sun, C. J. Li, B. L. Huang, Y. Yang, Y. J. Li, L. Wang and S. J. Guo, Intermetallic hcp-PtBi/fcc-Pt Core/Shell Nanoplates Enable Efficient Bifunctional Oxygen Reduction and Methanol Oxidation Electrocatalysis, *ACS Catal*., 2018, **8**, 5581-5590.

24 B. W. Zhang, Y. X. Jiang, J. Ren, X. M. Qu, G. L. Xu, S. G. Sun, PtBi intermetallic and PtBi intermetallic with the Bi-rich surface supported on porous graphitic carbon towards HCOOH electrooxidation, *Electrochim. Acta*, 2015, **162**, 254-262.

25 H. B. Liao, J. H. Zhu and Y. L. Hou, Synthesis and electrocatalytic properties of PtBi nanoplatelets and PdBi nanowires, *Nanoscale*, 2014, **6**, 1049-1055.

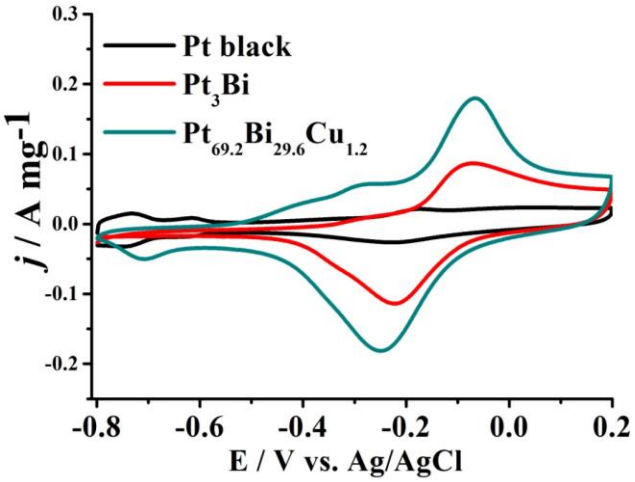

Fig. S3 CV curves of the $Pt_{69.2}Bi_{29.6}Cu_{1.2}$ nanoalloy, intermetallic Pt_3Bi nanocrystal and Pt black in 0.5M KOH. The sweep rate was 50 mV s^{-1}.

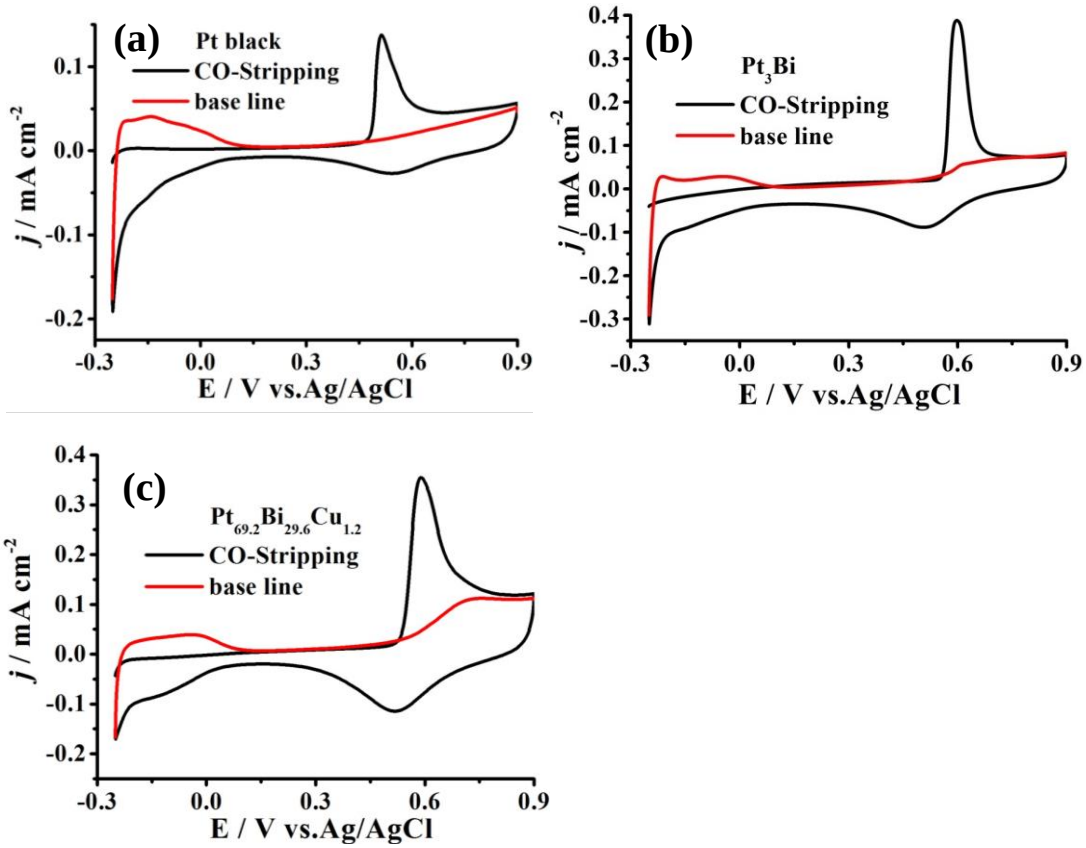

Fig. S4 CVs of CO stripping. (a) Pt black, (b) intermetallic Pt_3Bi nanocrystal and (c) $Pt_{69.2}Bi_{29.6}Cu_{1.2}$ nanoalloy.

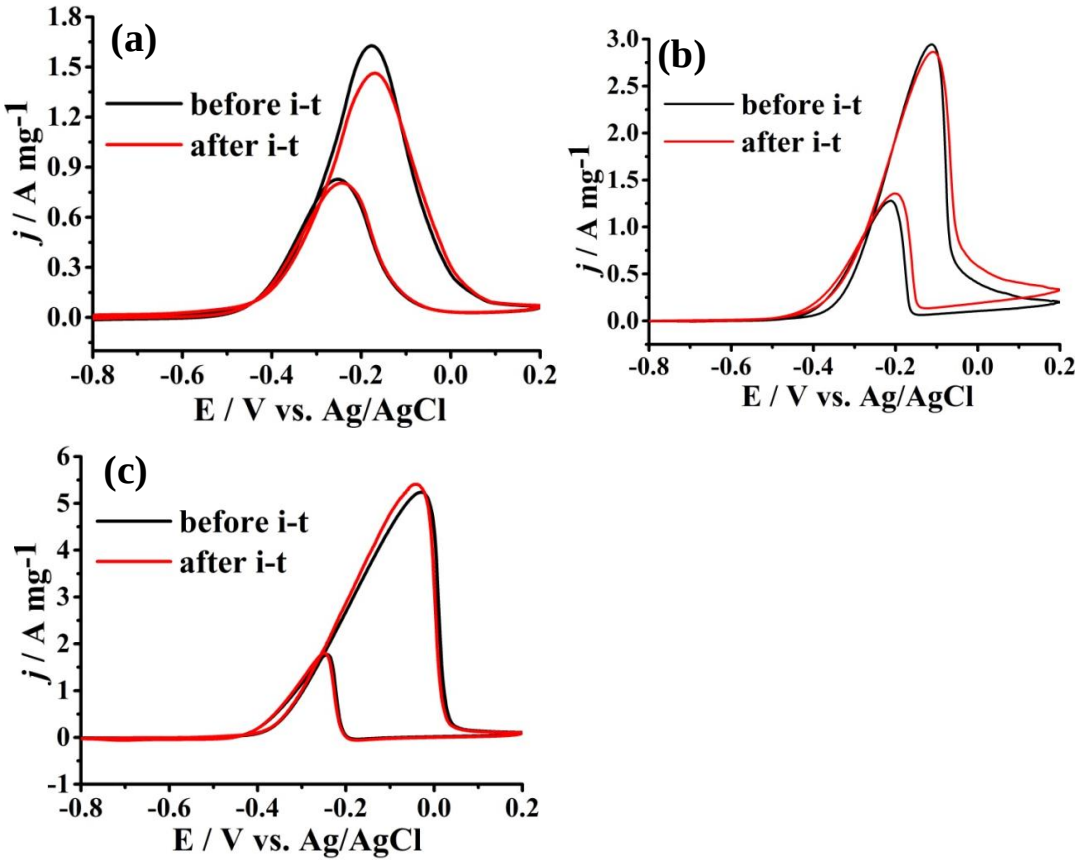

Fig. S5 Comparison of CVs of Pt black (a), intermetallic Pt_3Bi nanocrystal (b) and $Pt_{69.2}Bi_{29.6}Cu_{1.2}$ nanoalloy (c) in 0.5 M KOH+1 M CH_3OH before and after i-t test.

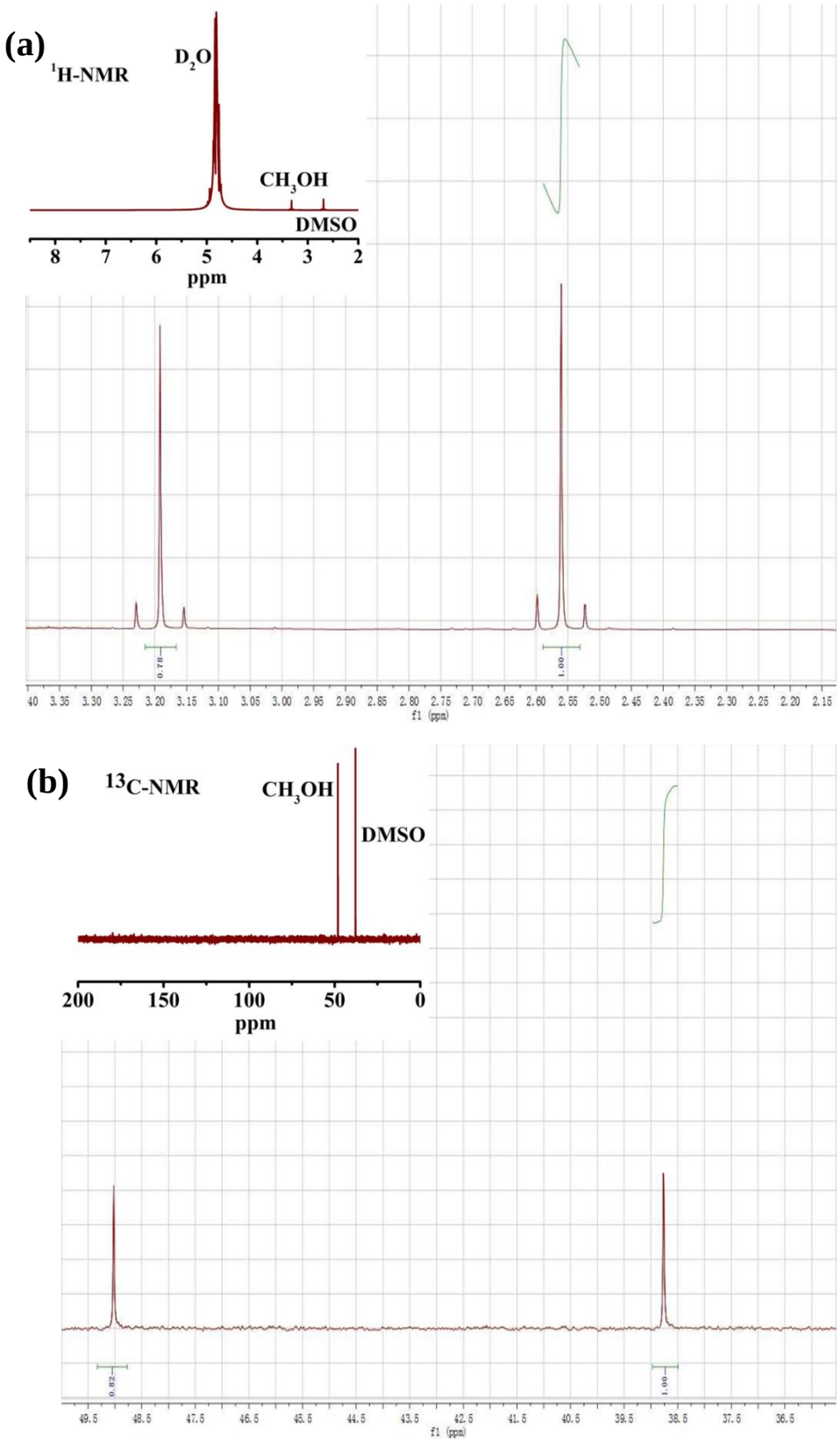

Fig. S6 The hydrogen spectrum (a) and carbon spectrum (b) of the solution after 30-hour test on $Pt_{69.2}Bi_{29.6}Cu_{1.2}$ nanoalloy.

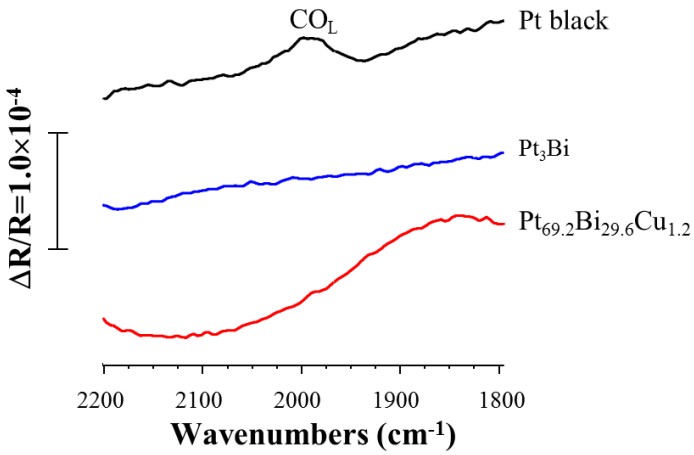

Fig. S7 In situ FTIR spectra between 2200 cm^{-1} and 1800 cm^{-1} of commercial Pt black, intermetallic Pt_3Bi nanocrystal and $Pt_{69.2}Bi_{29.6}Cu_{1.2}$ nanoalloy in 0.5 M KOH + 1 M CH_3OH solution at -0.7 V.

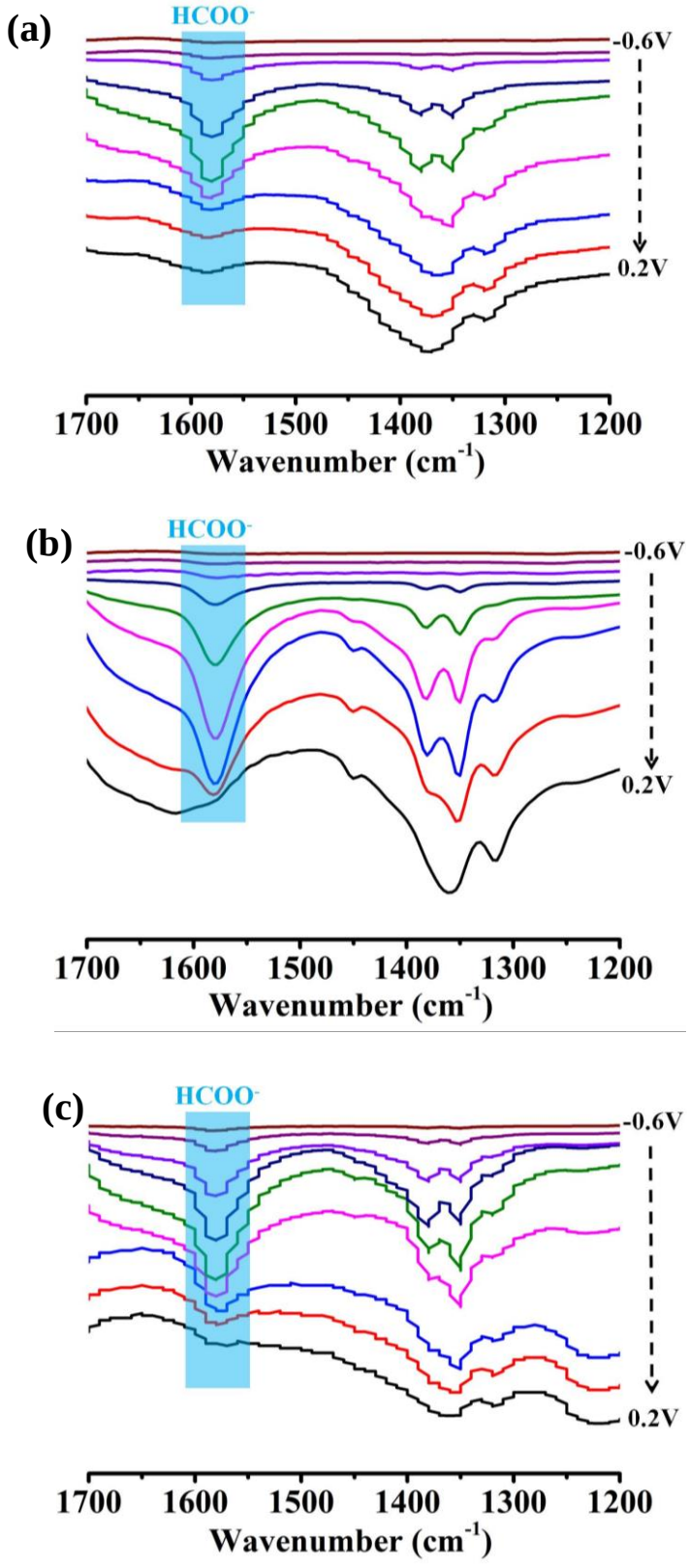

Fig. S8 In situ FTIR spectra between 1700 cm^{-1} and 1200 cm^{-1} of $Pt_{69.2}Bi_{29.6}Cu_{1.2}$ nanoalloy (a), intermetallic Pt_3Bi nanocrystal (b) and Pt black (c) in 0.5 M KOH + 1 M CH_3OH solution.